

# Thermally Induced Irreversible Conformational Changes in Collagen Probed by Optical Second Harmonic Generation and Laser-induced Fluorescence

T. Theodossiou<sup>1</sup>, G.S. Rapti<sup>1</sup>, V. Hovhannisyan<sup>2</sup>, E. Georgiou<sup>1</sup>, K. Politopoulos<sup>1</sup> and D. Yova<sup>1</sup>

<sup>1</sup>Biomedical Optics and Applied Biophysics Laboratory, Department of Electrical and Computer Engineering, Division of Electromagnetics, Electrooptics and Electronic Materials, National Technical University of Athens, Zografou, Athens, Greece

<sup>2</sup>Laboratory of Biomedical Optics, Applied R&D division, Yerevan Physics Institute, Yerevan, Armenia

**Abstract.** Irreversible thermal conformational changes induced to collagen have been studied by optical methods. More specifically, second harmonic generation (SHG) from incident nanosecond Ng:YAG 1064 nm radiation and laser-induced fluorescence by 337 nm, pulsed nanosecond nitrogen laser excitation, at 405, 410 and 415 nm emission wavelengths were registered at eight temperatures (40°, 50°, 55°, 60°, 65°, 70°, 75° and 80°C) and normalised with respect to the corresponding values at the ambient temperature of 30°C. The heating protocol used in this work, was selected to monitor only permanent changes reflecting in the optical properties of the samples under investigation. In this context, the SHG, directly related to the collagen fibril population in triple helix conformation, indicated on irreversible phase transition around 64°C. On the other hand fluorescence related to the destruction of cross-linked chromophores in collagen, some of which are related to the triple helix tertiary structure, also indicated a permanent phase transition around 63°C. These results are in agreement with previous results from studies with differential scanning calorimetry. However SHG and fluorescence, being non-invasive optical methods are expected to have a significant impact in the fields of laser ablative surgery and laser tissue welding.

**Keywords:** Collagen; Fluorescence; Gelatine; Second harmonic generation; Thermal denaturation

## INTRODUCTION

Several recent reports have dealt with optical harmonic generation in various types of biological tissue [1–7]. Collagen appears to be the common tissue component mainly responsible for these second order non-linear optical phenomena [2,4,5,7]. Collagen comprising about 6% of body weight in mammals, qualifies as the most widespread structural protein in higher vertebrates and the main means of their structural support. Its molecules consist of three amino acid chains convoluted in a rod-shaped, triple helix, and this tertiary structure of collagen is of microcrystalline triclinic nature, as demonstrated by the Bragg reflections in its X-ray diffraction pattern [8].

The fluorescence of collagen in the UV and visible spectral regions, has been investigated in many papers [9,10] and several attempts have been made to clarify its nature and origin [11,12]. The existence of at least four photolabile fluorescent chromophores found to absorb optical radiation in the region between 300 and 400 nm has also been shown [13]. In consequent work [14], several types of chromophores absorbing and emitting throughout the UVA and visible spectral regions were observed. Some collagen chromophores were isolated and identified as pentosidine and pyridinoline [10,12]. Both these chromophores are suggested to be products of cross-linking, pentosidine being age related. There are also various 'endogenous' chromophores in collagen found in the amino acid chains like tyrosine (fluorescence maximum at 303 nm) and phenylalanine (fluorescence maximum at 285 nm).

Correspondence to: Dr T. Theodossiou, 92 Ymittou st., 15561 Holargos, Athens, Greece. Tel: +301 6520717, e-mail: theo\_th@hotmail.com

Helix-coil transition in collagen induced by heating has been thoroughly studied [15–18]. More specifically it has been shown with the use of differential scanning calorimetry, that the position and shape of the denaturation endotherm of rat tail tendon collagen fibrils are governed by the kinetics of an irreversible process around 62°C, as shown by measurements of change of the specific heat capacity [15], whereas the thermal transitions of type I collagen were investigated again with the use of differential scanning calorimetry and spectrophotometry of turbidity, indicating an irreversible process centred around 52°C and corroborated by both methods used [16].

The thermal denaturation process in polar cod skin was investigated with the use of scanning microcalorimetry and intrinsic spectrofluorometry and was found to occur in three independent stages [17]. The effect of thermal denaturation on water collagen interactions were studied by use of NMR and differential scanning calorimetry [18] at four temperatures ranging from 40° to 70°C and the heat-induced structural changes were discussed.

In the current work second harmonic generation (SHG) from collagen and visible fluorescence are proposed as probes for the investigation of the degree of thermally induced denaturation. As SHG intensity is presumably proportional to the percentage of collagen molecules with triple helix of microcrystalline structure, it can directly indicate the denaturation ratio, i.e. the percentage of collagen fibrils in denatured form, lacking crystal structure and concomitant non-linear optical properties. Characteristics collagen fluorescence around the 410 nm spectral region on the other hand, induced by 337 nm nanosecond pulsed laser excitation, can be attributed mainly to cross-linked chromophores. Here both SHG and characteristic fluorescence of collagen at 405, 410 and 415 nm are suggested as non-invasive probes of irreversible thermal changes to the conformation of natural collagen. As SHG is dependent on the undenatured collagen fibrils it can relate directly to the denaturation ratio.

## EXPERIMENTAL PROCEDURE

Type I collagen from Achilles bovine tendon (Fluka 27662) in fibrous form was placed between glass microscope slides to form an almost uniform 1 cm × 1 cm square sample of less than 0.5 mm thickness. The microscope

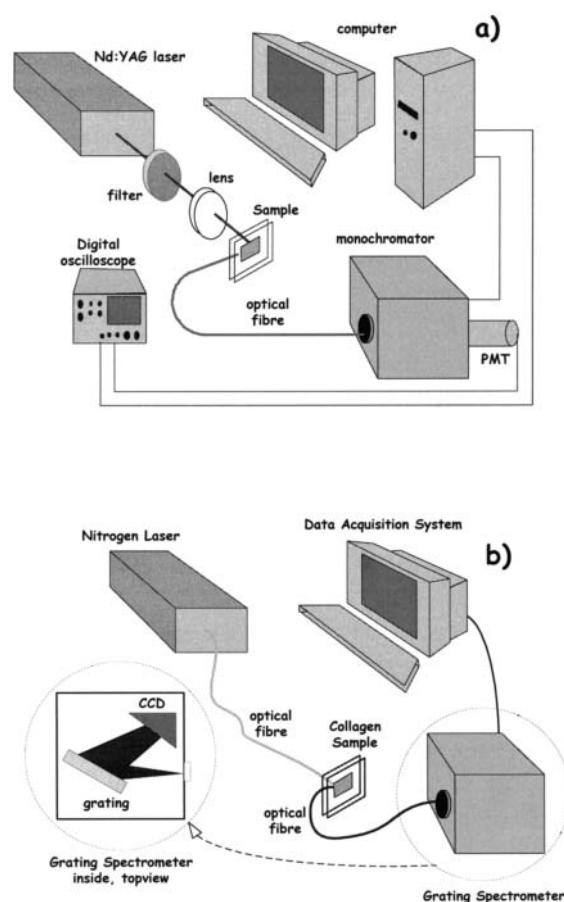


Fig. 1. Experimental set-up for (a) SHG measurements (b) characteristic fluorescence registration.

slides did not exhibit any absorption and emission in the spectral regions of interest (320–1100 nm). Quartz slides were avoided, as quartz is known to produce second harmonic radiation quite efficiently.

Sample preparation was based on a previously suggested protocol [18]. More specifically the samples were heated for 60 min in a water bath at temperatures ranging from 40 to 80°C (40°, 50°, 55°, 60°, 65°, 70°, 75° and 80°C). Each sample was then cooled to 4°C for 15 min. Finally the samples were brought to room temperature where all optical measurements were performed. In this manner only irreversible structural changes were investigated. Each sample also served as a control specimen, as it was immersed in water at 30°C for 60 min and then cooled to 4°C prior to heating to a specific temperature. Fluorescence spectra and SHG intensity value were registered for each individual sample both at the control temperature of 30°C and after heating according to the protocol.

The set-up for SHG measurements is shown in Fig. 1(a). A Nd:YAG pulsed Q-switched

Spectra Physics GCA 16 with 12 ns pulse duration was used as the source of 1064 nm radiation. The pulse energy  $E$  was set to 215 mJ. A lens with +75 mm focal length was used to focus the laser spot down to a 5 mm diameter circular spot on the sample surface. The interaction region was precisely marked for measurement repeatability after heating. A longpass filter cutting off at  $\lambda < 800$  nm was placed between the laser and the sample to reject spurious radiation (e.g. flashlamp originating). The resulting SHG signal was collected by a 600  $\mu\text{m}$ -diameter optical fibre at 45° angle to the incident beam and directed to an Optometrics SDMC1-03 grating monochromator set to 532 nm. At the exit of this monochromator an IR-blind Hamamatsu R4220 PMT insensitive to 1064 nm radiation produced an electronic signal which was then collected by a Tektronix TDS 540D digital oscilloscope, interfaced to a computer where the data were finally stored.

The SHG intensity was registered from each sample first at 30°C and then after heating to a specific temperature (40°, 50°, 55°, 60°, 65°, 70°, 75° and 80°C) and re-cooling according to the described protocol. The signal from each sample heat processed at a specific temperature as per our protocol was then normalised with respect to the signal obtained beforehand from the same sample at the control temperature of 30°C, to form the data set:

$$I_{\text{SHGnorm}} = \frac{I_{\text{SHG}}(T)}{I_{\text{SHG}}(30^\circ\text{C})} \quad (1)$$

The exponential errors in the case of the SHG signal, were of a statistical nature, in the form of the standard deviation of the mean value of the SHG signal obtained from each sample at the control temperature of 30°C, and were found to be of the order of 8%. These errors reflected the uncertainty in the signal intensity as measured and registered by our detection system.

The set-up for fluorescence registration is shown in Fig. 1(b). A Laser Science VSL-337ND nitrogen laser, with 4 ns pulse width operating at 30 Hz, delivered the excitation radiation of 0.3 mJ/pulse at 337 nm to a 0.8 cm diameter circular spot on the sample via a fused silica optical fibre with 600  $\mu\text{m}$  diameter. The same number of pulses were delivered to all the samples, summing to an overall incident energy per sample of 0.4 J. Again the excitation region was carefully marked for the

precise experiment repetition after sample heating. Another fused silica optical fibre with 1000  $\mu\text{m}$  core diameter collected the fluorescence and delivered it to the entrance of a 1024 CCD linear array grating spectrometer. A highpass filter, with cutoff at 350 nm, was placed there to reject any residual exciting radiation. The CCD was calibrated with respect to the wavelength with the use of a standard Ocean Optics HG-1 mercury-argon lamp, taking the advantage of its distinct spectral lines. The signal of the CCD was again stored in a computer interfaced to it via an A/D card.

From the collection of the fluorescence spectra at 30°C from all the collagen samples it is evident that we have a very good agreement in the spectral region between 405 and 420 nm. From this region where the signal to noise ratio is best, three wavelengths were selected, namely 405, 410 and 415 nm, at which analysis was carried out.

For each sample, elevated to a discrete temperature according to the protocol described above, the fluorescence intensities at these wavelengths were normalised with respect to the intensity at 30°C, to a new data set:

$$I_{\text{Fnorm}} = \frac{I_{\text{F}}(T)}{I_{\text{F}}(30^\circ\text{C})} \quad (2)$$

The experimental errors in the case of fluorescence registration were calculated in the same statistical manner as in the case of SHG signal registration. In this case they were found to be in the order of 10%.

In both SHG measurements and fluorescence registration the set-up geometry as well as experimental conditions were carefully maintained identical throughout the experiments.

The denatured counterpart of collagen, gelatine (Fluka 48722) in granular form, was used in an experiment aimed to explain some aspects of collagen fluorescence due to part of its cross-linked chromophores also existing in gelatine, as well as to illustrate reversible and irreversible changes due to heating as monitored by fluorescent registration.

The fourth harmonic of the Nd-YAG laser described earlier in the experimental section, was used according to the setup in Fig. 1(a) for the experiments with gelatine and was obtained by consecutive doubling (1064  $\rightarrow$  532 nm and 532  $\rightarrow$  266 nm) in two non-linear KDP crystals ( $\theta=41^\circ$  and  $\theta=78^\circ$ , *oo-e* interaction). The output parameters of the fourth

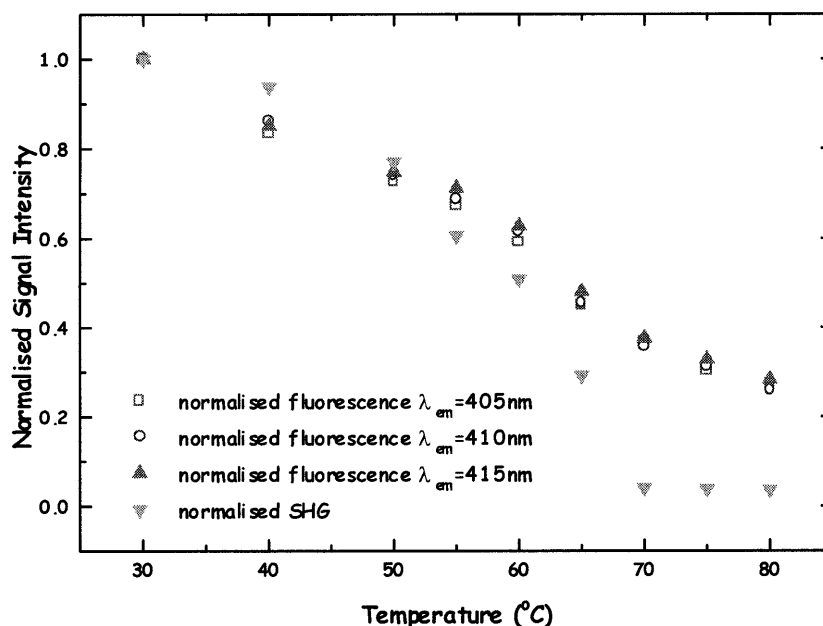


**Fig. 2.** The normalised SHG ( $1064 \rightarrow 532\text{ nm}$ ) values [ $I_{\text{SHGnorm}} = I_{\text{SHG}}(T)/I_{\text{SHG}}(30^\circ\text{C})$ ] of the collagen samples at eight temperatures as per the experimental protocol (▼) and the corresponding normalised fluorescence values [ $I_{\text{Fnorm}} = I_{\text{F}}(T)/I_{\text{F}}(30^\circ\text{C})$ ] for three emission wavelengths, 405 nm (□), 410 nm (○) and 415 nm (▲).

harmonic, used for UV excitation of tyrosine, were:  $\lambda = 266\text{ nm}$ ,  $E = 20\text{ mJ}$ . The fluorescent emission from this experiment was registered for the case of dry gelatine, gelatine in gel form after the addition of 10 ml bidistilled water and heating, and the same sample after drying in ambient temperature for two days.

## RESULTS

The SHG signal was registered as described in the experimental procedure first at  $30^\circ\text{C}$  and then after heating to a specific temperature and recooling. The signal from each sample likewise heat processed was then normalised with respect to the corresponding signal obtained for that specific sample at the control temperature of  $30^\circ\text{C}$  according to Equation (1). The results are shown in Fig. 2. In this plot the values at  $70^\circ$ ,  $75^\circ$  and  $80^\circ\text{C}$  can within experimental error be considered as zero.

Fluorescence measurements were again made with the set-up described in the previous section both at  $30^\circ\text{C}$  and each of the investigated temperatures. A characteristic collagen fluorescence spectrum can be seen in Fig. 3.

It can be seen that the maximum of this spectrum lies at  $395\text{ nm}$ . As also explained in the previous section due to the good signal-to-noise ratio in the spectrum region  $405\text{--}420\text{ nm}$ ,

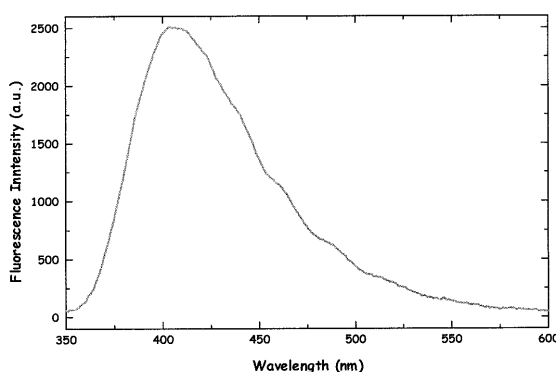


**Fig. 3.** Characteristic fluorescence from type I collagen from bovine Achilles tendon.

three wavelengths were selected from that region namely 405, 410, 415 nm for the analysis to be carried out. The fluorescence intensities at these wavelengths were normalised with respect to the intensity at  $30^\circ\text{C}$  forming a new dataset according to Equation (2).

The set of these data versus temperature is graphically presented for the three wavelengths along with the normalised SHG intensities in Fig. 2. From this figure it can be seen that the normalised SHG intensities and the normalised fluorescence intensities follow a similar pattern, however, the fluorescence data tend asymptotically to a value different than zero from  $70^\circ\text{C}$  upwards.

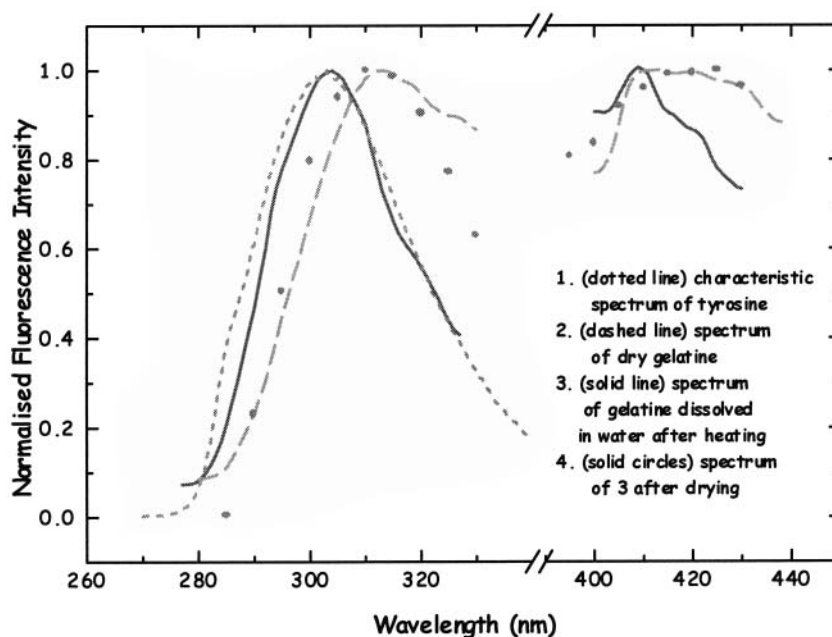


Fig. 4. Normalised spectra of gelatine fluorescence at 266 nm nanosecond Nd:YAG laser irradiation.

The results of the fluorescence registration experiments on gelatine, performed according to the description in the experimental procedure section, appear in Fig. 4. Curve 2 (dashed line) in Fig. 4 depicts the characteristic fluorescence of dry gelatine in granular form at ambient temperature. There is a maximum for that fluorescence at 314 nm and this is tyrosine-related fluorescence. However, the maximum is shifted with respect to curve 1 (dotted line) which depicts the fluorescence spectrum of tyrosine and has a maximum at 303 nm. The fluorescence around 410–420 nm of dry gelatine (curve 2 dashed line) is almost a plateau and the ratio of 410/420 nm values is practically one. The corresponding ratio of the maximum of tyrosine-like fluorescence over that at 420 for the same curve is 0.77. Curve 3 (solid line) on the other hand depicts the fluorescence of gelatine gel produced after addition of 10 ml bidistilled water to 2 mg dry gelatine and heating. The tyrosine-like spectral part of this matches almost exactly curve 1 with a maximum at 303 nm. Around the 410–420 nm region the spectral form is no longer a plateau but has a distinct maximum at 410 and a 410/420 nm value ratio of 1.2. The respective ratio of the tyrosine-like fluorescence at maximum over the value at 420 nm, is in this case approximately 1.

In curve 4 (solid circles) the fluorescence spectrum of the gel of curve 3 after drying in ambient temperature for two days, is

presented. The tyrosine-like fluorescence maximum is again shifted to longer a wavelength (311 nm) and the fluorescence at 410–420 nm tends to a plateau again, with a ratio of values at 410/420 nm of 0.95. The ratio of the maximum of the tyrosine-like fluorescence over the value at 420 nm is 0.75.

## DISCUSSION

SHG in collagen originates mainly from collagen macroscopic polymerised fibrils and their microcrystal structure, which is dependent on triple helix conformation. Gelatine, which has a similar chemical composition to collagen but lacks its tertiary structure, both at the molecular and fibril level does not exhibit any detectable SHG.

Unlike inorganic non-linear crystals, collagen fibrils have isotropic distribution and orientation. Hence the resulting SHG emission is also isotropic (non-directional) and is not governed by phase matching conditions but depends on the coherence length between the fundamental and second harmonic radiation components [2]. This being the case, if collagen fibrils have a diameter smaller or comparable to this effective length, then the second harmonic radiation emitted is proportional to the fibril population in triple helix conformation. On the other hand if the fibril diameter is bigger than the coherence length the above

proportionality is violated. In our experiments since the SHG measurements are taken in the reflection geometry, it can be safely assumed to be proportional to the fibril population in triple helix form. The normalised second harmonic intensity of Fig. 2 with respect to the 30°C denotes the percentage of collagen molecules remaining in triple helix form in a given protocol temperature with respect to the temperature of 30°C.

In this context SHG emerges as a powerful probe of the degree of thermal denaturation of the bovine Achilles tendon type I collagen under investigation. The fact that the values of this curve are practically zero at 70°C and above, indicates complete denaturation of our sample at these temperatures. In the same graph (Fig. 2) the curves of fluorescence vs. temperature appear at the three emission wavelengths selected, namely 405, 410 and 415 nm. It can be readily seen that the fluorescence curves are in very good agreement with each other; however between 70 and 80°C unlike the SHG curve there is some residual fluorescence still undergoing thermal quenching but at a different rate. In natural form collagen has a number of chromophore cross-links that emit around the 400 nm spectral region. A big part of them is related to the triple helical structure of the collagen and its fibrils, so when collagen undergoes thermal denaturation these cross-links are destroyed. However, random cross-links remain in collagen between individual amino acid strands even after complete denaturation. These random cross links are also present in gelatine, the denatured counterpart of collagen and are responsible for its characteristic fluorescence in the visible region. It must, however, be noted that upon heating of gelatine in an aqueous environment, these cross-links are destroyed and their characteristic fluorescence is quenched. Upon registration of this fluorescence with 266 nm nanosecond 20 mJ/pulse irradiation, as detailed in previous sections, it was shown that whereas the cross-link-originating fluorescence was quenched, the endogenous (mainly tyrosine) fluorescence rose and this effect was reversible after water evaporation at ambient temperature (Fig. 4).

The results of the experiment on gelatine, can lead us to conclude that a part of gelatine related cross-link chromophores exist in tissue even after complete thermal denaturation and continue to undergo thermal damage some of

which is reversible. This fact accounts for the residual tail appearing in the fluorescence data of Fig. 2. It can further be suggested that the chromophore species emitting around 420 nm, is tyrosine-related and could be dityrosine or polytyrosine as proposed elsewhere [13].

However, various other cross-link-chromophores, such as pentosidine or pyridinoline found to exist in collagen fluorescence around the 400 nm spectral region under UVA excitation [10,13]. All cross-link-chromophores of collagen are destroyed upon thermal denaturation and this is a result of the helix coil transition as the amino acid strands become detached from one another. For some of these chromophores this process is irreversible whereas for others it is reversible to a certain extent (e.g. gelatine-associated cross-links) as shown above.

Figure 5 shows the differentials of the four curves of Fig. 2, with their sign changed so that the biggest rate of destruction corresponds to a maximum instead of a minimum. Curve 1 depicts the differential of the SHG signal of Fig. 2 with temperature. Curves 2, 3 and 4 show the corresponding differential curves of collagen fluorescence vs. temperature for the three selected wavelengths 405, 410 and 415 nm, respectively. Curve 1 starts rising at about 36°C monotonically, indicating a constantly increasing rate of permanent destruction of triple helix formations in collagen, up to about a temperature of 55°C. From this temperature upward, there is an even steeper increase of the rate of destruction up to 64°C where there is a maximum. Following that there is a very steep decrease of the rate of helix-coil transition up to about 75°C where the rate becomes zero due to complete denaturation of our sample.

Since our experimental protocol was designed to detect permanent changes in collagen, this further indicates practically an irreversible phase transition centred about 64°C of collagen into gelatine. The fluorescence curves on the other hand practically show a steady destruction of fluorophores from 30 to 55°C which indicates recombination of some destroyed fluorophores and that is why the curve is not in complete agreement with the corresponding curve of SHG in that region. From 55 to 77°C, however, there is a notable increase in the permanent destruction of collagen fluorophores which reaches a maximum at about 63°C and then drops again to a steady

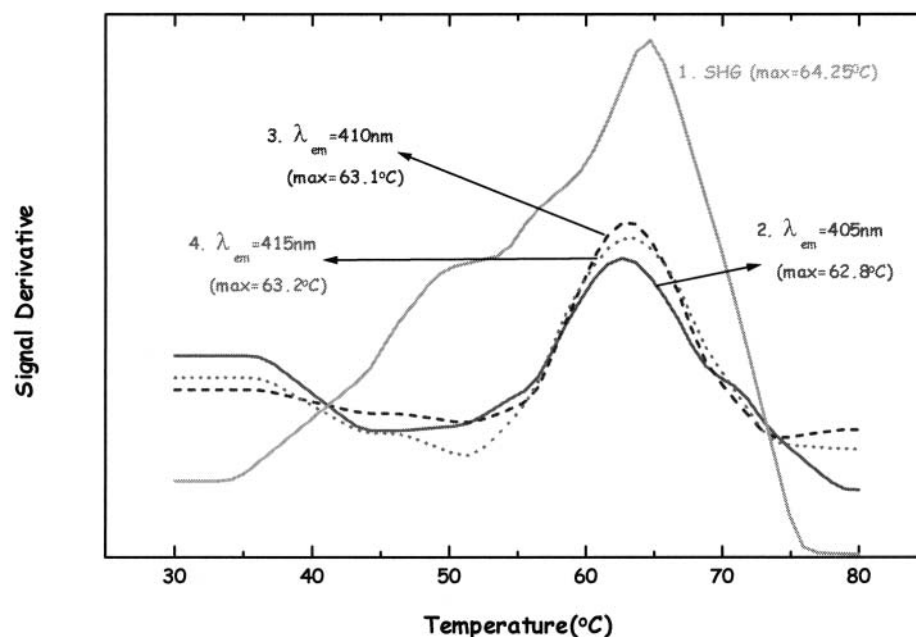


**Fig. 5.** Differential curves of the data in Fig. 2 with inversed sign so that maximum corresponds to biggest rate of irreversible thermal destruction of triple helix population in the case of SHG and cross-link chromophores in the case of fluorescence at the three emission wavelengths.

state of destruction of the residual collagen fluorophores after complete denaturation.

Both the SHG and fluorescence differential curves show a phase transition of collagen centred around 63–64°C, into its denatured form, which is in complete agreement with previous experimental results from differential calorimetry [15,16]. In Tiktopulo and Kajava [16] the phase transition point (52°C) is different from that of the present work (63–64°C) and that of Miles et al. [15] (62°C). This can be explained by the fact, that skin tissue was used which is expected to have a lower phase transition point than tendon tissue, as used in the two later cases.

The SHG measurements presented here are more sensitive to thermal damage of tissue since they directly monitor destruction of triple helix of fibril formations in tissue. Fluorescence on the other hand, can be induced by quite low energy density of incident radiation due to its one photon nature but cannot directly associate with the thermal denaturation. Instead it measures chromophore destruction, a part of which is reversible. In addition, photobleaching of the chromophores during resonant irradiation is an important factor that might affect measurements in vivo. The present experiments, however, where photobleaching was negligible, show that a part of the tissue cross-linked

chromophores associated to triple helix fibrils, undergo permanent damage and are thus capable of reflecting irreversible phase transitions during tissue thermal denaturation.

In the current work, experiments designed to register irreversible changes to type I collagen from Achilles bovine tendon, showed that both SHG and fluorescence (optical non-invasive methods unlike calorimetry) have successfully demonstrated thermally induced phase transitions around the temperature of 64°C.

This result can prove invaluable to laser ablative surgery, where the condition and permanent conformational changes to the tissues surrounding the ablation area can be probed in vivo. Another field where the current work can be applied to, is laser tissue welding where it is important to know when phase transition has been achieved, so that further irradiation and consequently thermal damage can be avoided.

## REFERENCES

1. Fine S, Hansen WP. Optical Second harmonic generation in biological systems. *Appl Opt* 1971;10:2350–3.
2. Freund I, Deutch M, Sprecher A. Connective tissue polarity. Optical second-harmonic microscopy, crossed-beam summation, and small-angle scattering in rat-tail tendon. *Biophys J* 1986;50:693–712.

3. Guo Y, Ho PP, Tirkšliunas A, Liu F, Alfano RR. Optical harmonic generation from animal tissues by the use of picosecond and femtosecond laser pulses. *Appl Opt* 1996;35:6810–13.
4. Theodossiou T, Georgiou E, Hovhannisyan V, Yova D. Visual observation of infrared laser speckle patterns at half their fundamental wavelength. *Lasers Med Sci* 2001;16:34–9.
5. Yova D, Theodossiou T, Hovhannisyan V. Photo-induced effect of hypericin on collagen and tissue with high collagen content. *SPIE Proc* 1999;3565:174–80.
6. Hovanesian V, Lalayan A. Second harmonic generation in biofiber-containing tissues. *Proc Int Conf On Lasers '96*, Portland, OR, 1996:107–9.
7. Georgiou E, Theodossiou T, Hovhannisyan V, Politopoulos K, Rapti GS, Yova D. Second and third optical harmonic generation in type I collagen, by nanosecond laser irradiation, over a broad spectral region. *Opt Comm* 2000;176:253–60.
8. Fraser RDB, Macrae TP. The crystalline structure of collagen fibrils in tendon. *J Mol Biol* 1979;127:129–33.
9. Burshtein EA. Autoluminescence of Proteins (Nature and Applications). Moscow: VINITI AN SSSR (series 'Biofizika', in Russia), 1977.
10. Uchiyama A, Ohishi T, Takahashi M, Kushida K, Inoue T, Fuijeand M, et al. Fluorophores from aging human cartilage. *J Biochem* 1991;110:714–18.
11. Volkov AS, Kumekov SE, Syrgaliev EO, Chernyshov SV. Photoluminescence and anti-Stokes emission of native collagen in visible range of spectrum. *Biofizika* 1991;36:770–3.
12. Fujimoto D, Akiba K, Nakamura N. Isolation and characterization of a fluorescent material in bovine Achilles tendon collagen. *Biochem Biophys Res Commun* 1977;76:1124–9.
13. Menter JM, Williamson JD, Carlyle K, Moore CL, Willis I. Photochemistry of type I acid soluble calf skin collagen. Dependence of excitation wavelength. *Photochem Photobiol* 1995;62(3):402–8.
14. Yova D, Hovhannisyan V, Theodossiou T. Photochemical effects and hypericin photosensitized processes in collagen. *J Biomed Opt* 2001;6:52–57.
15. Miles CA, Burjanadez TV, Bailey AJ. The kinetics of the thermal denaturation of collagen in unrestrained rat tail tendon determined by differential scanning calorimetry. *J Mol Biol* 1995;245:437–46.
16. Tiktopulo EI, Kajava AV. Denaturation of type I collagen fibrils is an endothermic process accompanied by a noticeable change in the partial heat capacity. *Biochemistry* 1998;37:8147–52.
17. Shnyrov VL, Lubsandirzhieva VC, Zhadan GG, Permyakov EA. Multi-stage nature of the thermal denaturation process in collagen. *Biochem Int* 1992;26:211–17.
18. Rochdi A, Foucat L, Renou JP. Effect of thermal denaturation on water collagen interactions: NMR relaxation and differential scanning calorimetry analysis. *Biopolymers* 1999;50:690–6.

*Paper received 2 February 2001;  
accepted after revision 7 May 2001.*